Threshold singularities of the x-ray Raman scattering in metals

Philippe Nozières*
Institut Laue-Langevin, Cedex 156, 38-Grenoble, France

Elihu Abrahams†
Physics Department, Rutgers University, New Brunswick, New Jersy 08903

(Received 22 April 1974)

We study the theory of x-ray Raman scattering involving the virtual excitation of a deep-core-state hole in a metal. In the intermediate state the conduction electrons experience a transient potential due to the temporary appearance of the core hole; the resulting "final state" interactions determine the singular behavior of the scattering rate near threshold just as they do in x-ray absorption or emission. This is described using a time representation of perturbation theory in the Kjeldysh formalism which permits an exact determination of the power law of the threshold singularities. We discuss the role of lifetime effects and the distinction between scattering and fluorescence. We discuss at length the role of interference between different intermediate localized core hole sites. If we neglect interference effects we can give an expression for the scattering rate which is suitable for computing. We are unable to solve the coupled Dyson equations when interference is included; in that case we give only qualitative results and discuss the interplay of interference and lifetime effects, especially in the fluorescence case where the final-state interactions tend to destroy interference in the long-lifetime limit.

I. INTRODUCTION

A. Specification of the problem

We consider a typical electronic Raman x-ray scattering process in a metal, in which an incoming x-ray of frequency and wave vector $(\omega, \vec{q})$ is scattered into the state $(\omega', \vec{q}')$. The extra energy and momentum is transferred to some electronic excitation of the conduction electrons. Let $W_{qq'}(\omega, \omega')$ be the corresponding transition probability. The coupling of the electrons to the photons is described by the usual semiclassical Hamiltonian

$$H_{\rm int} = \int d\tau \left(\frac{e}{c} \vec{j} \cdot \vec{A} + \frac{e^2}{2mc^2} \rho A^2 \right) , \tag{1}$$

where $\vec{A}$ is the vector potential of the x-ray field, and ρ and $\vec{j}$ are the number and current densities of the conduction electrons.

The Raman-scattering matrix element arises either from the A^2 term of Eq. (1) treated in first order or from the $\vec{j} \cdot \vec{A}$ term treated to second order. For free electrons, the former process is usually dominant and the linear term is ignored.[1] If, however, ω lies close to an absorption threshold then the $(\vec{j} \cdot \vec{A})^2$ process will display a resonance and it may eventually dominate the usual ρA^2 matrix element.

To estimate the relative order of magnitude of the two contributions, consider a nearly elastic process in a free-electron gas in which an electron in state $\vec{k}$ below the Fermi surface is scattered to the state $\vec{k}' = \vec{k} + \vec{q} - \vec{q}'$ outside. This may occur either directly through the ρA^2 term [Fig. 1(a)] or via a more or less localized deep-core state c with the $\vec{j} \cdot \vec{A}$ term acting twice [Fig. 1(b)]. In the former case, the matrix element is simply $\Lambda_1 = e^2 A^2 / 2m^2 c^2$, while for the latter case it is

$$\Lambda_2 = \frac{(e\vec{j} \cdot \vec{A}/c)_{kc} (e\vec{j} \cdot \vec{A}/c)_{ck'}}{\omega - \epsilon_k + \epsilon_c} . \tag{2}$$

Qualitatively, we may relate the matrix elements of $\vec{j}$ to the oscillator strength f_c between the core state and the conduction band

$$j_{kc} j_{ck'} \approx f_c(\epsilon_k - \epsilon_c)/m .$$

Then,

$$\frac{\Lambda_2}{\Lambda_1} \approx \frac{f_c(\epsilon_k - \epsilon_c)}{\omega - \epsilon_k + \epsilon_c} . \tag{3}$$

If ω is near the absorption threshold, then $\omega - \epsilon_k + \epsilon_c$ is small and Λ_2 is dominant—the usual *resonant Raman scattering*. For free electrons, Λ_1 dominates, since the level c would then be in the conduction band, in which case $\omega \gg \epsilon_k - \epsilon_c$ and Λ_2 may be neglected.

In this paper we shall only be concerned with

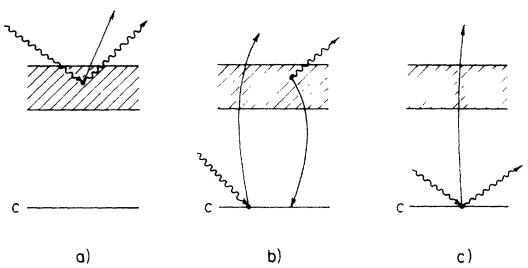

FIG. 1. Raman-scattering processes in metals.

resonant scattering in which both ω and ω' lie close to an absorption threshold. The core state only enters as an intermediate step; the final state involves excitation of conduction electrons only. The transition probability is then controlled by the $\vec{j}\cdot\vec{A}$ coupling [as in Fig. 1(b)]. These processes should not be confused with Raman scattering of an electron from a core state into the conduction band [Fig. 1(c)]. Such processes, discussed by Doniach, Platzman and Yue[1] arise mostly from the ρA^2 coupling in Eq. (1). They are of a completely different nature than the ones we are considering.

B. Scattering and fluorescence: Lifetime effects

We now focus our attention on a metal at zero temperature. To the extent that we may ignore lifetime broadening, the absorption and emission spectra possess sharp thresholds

$$\omega_0 = \epsilon_F - \epsilon_c \ , \tag{4}$$

where ϵ_F is the Fermi energy. The threshold may be shifted by final-state interactions; we shall return to this point later. If $\omega' < \omega < \omega_0$, the intermediate state in Fig. 1(b) is necessarily virtual (the first absorption process cannot conserve energy), the effective matrix element Eq. (2) is then finite and there is no ambiguity in calculating the transition probability $W(\omega, \omega')$. The same conclusion holds if $\omega_0 < \omega' < \omega$ (the second emission process cannot conserve energy). On the other hand, if $\omega' < \omega_0 < \omega$, difficulties occur. It is then possible to have two successive *real* transitions, absorption followed by emission. If we do not introduce a finite lifetime for the intermediate state, we should find that $W(\omega, \omega')$ is infinite. As usual, the difficulty can be cured by using a Weisskopf-Wigner version of perturbation theory in which a finite lifetime τ of the intermediate state is explicitly taken into account. This lifetime may arise from the radiative emission process itself but in our problem it will always be controlled by nonradiative Auger decay of the deep core state. In any case, the finite lifetime introduces an imaginary part $i/2\tau = i\Gamma$ into the energy denominators, thus curing divergences. Another consequence of the lifetime is to blure the transition probability over a range Γ; the sharp thresholds at ω_0 are broadened. If we are far from threshold, i.e.,

$$\omega - \omega_0, \ \omega_0 - \omega' \gg \Gamma \ , \tag{5}$$

then we may argue that the intermediate state builds up for a time τ at a rate $W_A(\omega)$, the absorption transition probability. It then reradiates at the emission rate $W_E(\omega')$ and we find

$$W(\omega, \omega') = \tau \ W_A(\omega) \ W_E(\omega') \ . \tag{6}$$

Rather than a genuine Raman scattering, we then have a *fluorescence* process, with two *real* transitions, the interplay of which is controlled by the lifetime τ.

The influence of the finite lifetime of the deep core hole has been studied by several authors. Yue and Doniach[2] were interested in x-ray production by electron bombardment (as in usual anticathodes). They showed that because the energy need not be conserved exactly in the intermediate state, the emission spectrum extends beyond the threshold. They were mostly concerned with the transition region $\omega' - \omega_0 \sim \Gamma$ and with a discussion of the spectrum shape. McMullen and Bergersen[3] studied the influence of Γ in detail by a method similar to the one we use here; they too were mostly interested in the shape of the transition region (they discuss for instance the validity of the Weisskopf-Wigner procedure of convoluting the imperturbed spectrum with a Lorentzian of width Γ).

C. Summary of the paper

In this paper, we shall not consider the blurring effect of the core-hole lifetime. We stay out of the transition region and always assume the conditions Eqs. (5). We want to calculate the genuine Raman scattering rate $W(\omega, \omega')$ when $\omega\omega' > 0$. As a by-product we shall check that in the case $\omega' < \omega_0 < \omega$ it takes the form in Eq. (6). We shall then discuss various features of the results both for Raman scattering and fluorescence. We shall not attempt to find the exact shape in the transition region.

Let w_k be the matrix element for x-ray absorption with excitation of an electron from the core to the conduction-band state k. If we entirely neglect Coulomb interactions and lifetime effects, then the transition probability is

$$W(\omega, \omega') = 2\pi \sum_{kk'} n_{k'}(1 - n_k) \times \left| \frac{w_k w_{k'}}{\omega - \epsilon_k + \epsilon_c} \right|^2 \delta(\omega - \omega' - \epsilon_k + \epsilon_{k'}) \ . \tag{7}$$

Note that if $\omega' < \omega_0 < \omega$ the energy denominator passes through 0 and W becomes infinite. In this paper we wish to study the effect of "final-state" interactions between the conduction electrons and the deep hole on $W(\omega, \omega')$. Although these actually occur in the *intermediate* state in the presence of the core hole, we shall use the nomenclature "final-state" interactions. In the case of x-ray absorption or emission, it is known that such effects give rise to the so-called "infrared singularities" in the vicinity of threshold.[4] Similar effects should occur in the scattering: We shall see that when $|\omega - \omega_0|$ and/or $|\omega' - \omega_0|$ are small, W behaves as

$$W(\omega, \omega') \approx \frac{1}{|\omega - \omega_0|^n} f\left(\left|\frac{\omega' - \omega_0}{\omega - \omega_0}\right|\right),$$

where n is a "critical exponent" and f a universal function that can be fully explicated in some cases. This problem has already been studied by Ting, Birman, and Abrahams[5] in the weak-coupling limit using the machinery of perturbation theory and parquet diagrams. Here we wish to use the more powerful method of Nozières and deDomenicis[6] based on a time (rather than energy) representation of perturbation theory. The exponent n can thus be obtained exactly and the physical interpretation is far more obvious.

The plan of the paper is as follows: In this Introduction, we have defined the problem in a very qualitative way and exposed the importance of lifetime effects and the relationship between Raman scattering and fluorescence. In Sec. II we introduce the formalism we shall use and we develop it to elucidate the role of interference effects involving core holes created at different sites.

In Sec. III, an exact calculation of the transition rate, valid near threshold but outside the transition region, is carried out neglecting interference effects. The problem is then much simplified since the system retains full rotational symmetry around the core hole in the intermediate state; the different angular-momentum channels may be decoupled. Infrared singularities are explicitly displayed, both for Raman scattering and fluorescence. This section is a generalization of the previous work of Ref. 5.

In Sec. IV, the interference effects are considered in detail. The coupled transient Dyson equations which describe the final-state interactions are easily found but unexpectedly cannot be solved. We are restricted to a study of the contribution of the simplest excitations; this allows a qualitative physical discussion of the nature of interference effects in both Raman scattering and fluorescence.

We emphasize that the theory of Raman scattering and fluorescence is well established. One purpose of this paper is to look at it in a rather unusual way in order to display physical effects which are often hidden in elementary formulations.

II. FORMALISM

A. Kjeldysh-Schwinger perturbation theory

We now develop the machinery to carry out the calculation of Raman scattering in metals using the time representation of perturbation theory. The effects of interference between intermediate states having core holes at different sites will then be easily identified. The calculation is most easily carried out using the Kjeldysh-Schwinger[7] form of perturbation theory; it is particularly convenient for obtaining transition probabilities. Also, such a nonequilibrium formulation is well suited for the introduction of lifetime effects. A similar formalism has been used in Refs. 2 and 3.

We write the Hamiltonian of the electron system as[4]

$$H = \sum_k \epsilon_k c_k^\dagger c_k + \epsilon_c d^\dagger d + \sum_{kk'} V_{kk'}\, c_k^\dagger c_{k'}\, dd^\dagger . \tag{8}$$

Here $c^\dagger$, $d^\dagger$ are creation operators for a conduction electron and a core electron, ϵ_c is the core state energy. $V_{kk'}$ is the final state scattering potential, present only when the core state is empty. We set the origin of energy at the Fermi level. The absorption/emission threshold is then $\omega_0 = -\epsilon_c$ in the absence of the interaction $V_{kk'}$. The coupling to the x-ray field is described by[4]

$$H_x = \sum_k \omega_k c_k^\dagger d + \text{c.c.} .$$

At time $t = -\infty$ we start from the state $\alpha_q^\dagger |0\rangle$, where $|0\rangle$ is the electron ground state (core state filled) and $\alpha_q^\dagger$ is the incoming photon creation operator. To second order in H_x, the wave function at time t_0 is

$$|\psi_q(t_0)\rangle = -\int_{-\infty}^{t_0} du \int_{-\infty}^{u} dt \times U(t_0, u)\, H_x\, U(u, t)\, H_x U(t, -\infty)\, \alpha_q^\dagger |0\rangle , \tag{9}$$

where $U(t, t')$ is the time evolution operator when $H_x = 0$. The probability of finding a photon q' at time t_0 for an arbitrary conduction electron state is

$$P_{qq'} = \langle \psi_q(t_0) | \alpha_{q'}^\dagger \alpha_{q'} | \psi_q(t_0) \rangle . \tag{10}$$

The transition probability is then simply $dP_{qq'}/dt_0$.

We calculate $P_{qq'}(t_0)$ in the Kjeldysh-Schwinger formalism in which chronological products are ordered from $t = -\infty$ to $t = +\infty$ and back. We then have a forward (upper) time branch on which all the interactions in the ket $|\psi_q(t_0)\rangle$ in Eq. (10) take place. The interactions in the bra $\langle \psi_q(t_0)|$ are on the backward (lower) time branch. The diagram for $P_{qq'}(t_0)$ as defined in Eqs. (9) and (10) is shown in Fig. 2, where the wavy lines are photons, and full and dotted lines are respectively conduction and core electrons. The bubble contains vertices on the upper and lower time branches all interconnected by conduction electron lines. Each full line that joins an upper vertex to a lower one corresponds to a real excitation created in the Raman-scattering process. The half of the the diagram containing the upper vertices may be viewed as the scattering *amplitude* for a given final state described by the lines joining the upper and lower halves. (Upward lines represent excited conduction holes, downward lines represent excited elec-

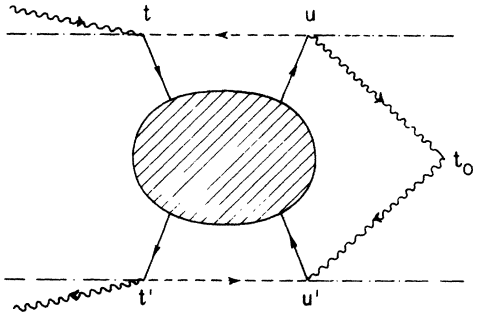

FIG. 2. Structure of diagrams for the transition probability in the Kjeldysh formalism. Wavy lines, photons; full lines, conduction electrons; dotted lines depict the deep hole.

trons). The whole diagram describes the transition *probability* with due account of interference effects. A complete exposition of the formalism may be found in Kjeldysh's paper.[7]

B. Transition probability

Let us first disregard the space variables; we consider only the time variables in Eqs. (9) and (10). In the calculation of $\alpha_{q'}|\psi_q(t_0)\rangle$ on the upper branch of Fig. 2, the photons contribute a factor $e^{i\omega' u - i\omega t}$ apart from a constant phase. Likewise, the deep hole is a sharp state and has the propagator $e^{i\epsilon_c(u-t)}$ on the upper branch. Therefore, in the calculation of $|\psi_q(t_0)\rangle$ [Eq. (9)], we may replace U by the evolution operator for the conduction electrons only in the presence of the transient scattering potential of the deep hole established between t and u. Let us measure the photon frequencies ω, ω' from the threshold $\omega_0 = -\epsilon_c$ so that when we combine the phase factors from photon and deep-hole propagators for both time branches we get, for the probability,

$$P_{qq'} = \int_{-\infty}^{t_0} du\, du' \int_{-\infty}^{u} dt \int_{-\infty}^{u'} dt' \times S(t, u, u', t')\, e^{i\omega(t'-t)}\, e^{-i\omega'(u'-u)}, \qquad (11)$$

where $S(t, u, u', t')$ is the contribution of all the conduction electron lines and electron-hole vertices in Fig. 2.

The transition rate is obtained by deriving $P_{qq'}$ with respect to t_0. This is equivalent to fixing one time, say $u = 0$ and integrating the others without restriction. Thus

$$W(\omega, \omega') = \int_{-\infty}^{+\infty} du' \int_{-\infty}^{0} dt \int_{-\infty}^{u'} dt' \times S(t, 0, u', t')\, e^{i\omega(t'-t)}\, e^{-i\omega' u'}. \qquad (12)$$

The calculation of W is thereby reduced to a purely electronic problem.

C. Interference effects

We return to the space variables previously omitted. During the scattering process, the intermediate core hole is created at some atomic site i. In the sum over intermediate states interference terms will occur between x-rays scattered from different sites. This will be reflected in Fig. 2 by the core holes of the upper and lower time branches being created at different sites. Note that such an interference still exists even in the case of fluorescence, a somewhat puzzling conclusion to which we return later. The electronic kernel S of Eq. (12) depends on two space variables (i, j) essentially through the electron lines that cross from top to bottom. (The upper vertices scatter at R_i, the lower at R_j.) Suppose downward lines have momenta $\vec{k}_\alpha$ and upward lines $\vec{k}'_\alpha$. Then S_{ij} contains a factor

$$\exp\left(i \sum_\alpha (\vec{k}_\alpha - \vec{k}'_\alpha) \cdot (\vec{R}_i - \vec{R}_j)\right). \qquad (13)$$

The transition rate is obtained by summing (i, j) taking account of the phases of the photon lines:

$$W_{qq'}(\omega, \omega') = \sum_{ij} W_{ij}(\omega\omega')\, e^{i(\vec{q}-\vec{q}')\cdot(\vec{R}_i - \vec{R}_j)}. \qquad (14)$$

Equations (13) and (14) guarantee overall momentum conservation—a conclusion which actually relies on the interference process.

In order to ascertain the range of the interference, we note that each line between the top and bottom branches of Fig. 2 provides a factor of order $|R_{ij}|^{-1}$ (the electron propagator in configuration space). Then two cases are possible. If in the final state more than one electron and one hole is excited (at least two upward and two downward lines in Fig. 2), the summation over $\vec{R}_{ij}$ in Eq. (14) converges naturally and has an atomic range. The photon momenta $\vec{q}$ and $\vec{q}'$ are usually small compared to the Fermi momentum and the photon phase factor in Eq. (14) may be ignored. For this case, the space coordinate representation is more convenient than the momentum representation. Indeed, the single term $i = j$ (no interference) provides an estimate of W which is not ridiculous. On the other hand, if only one electron (and one hole) is excited, the situation is completely different. W_{ij} then varies as $|R_{ij}|^{-2}$ and the range of interference is controlled by the photon momentum transfer $|\vec{q} - \vec{q}'| = \Delta q$; it is of order $1/\Delta q$, much larger than atomic size. In this case, the interference is a dominant feature and the usual momentum representation is more convenient than the use of site coordinates i, j.

The one-particle–one-hole excitation final state is special in another way. Since the momentum transfer is to a single electron, the maximum en-

ergy transfer $\Delta\omega = \omega - \omega'$ is $v_F \Delta q$ (in the multiple excitation case, $\Delta\omega$ is not limited). For soft x-rays, Δq is small and the single particle excitation scattering will be lost in the transition region of width Γ near threshold. Moreover, the corresponding integrated intensity, which at first sight might seem to be enhanced by a factor $1/\Delta q$ because of more extensive interference, is actually reduced because both the electron and the hole must be close to the Fermi surface. For intermediate coupling, the single excitation process is actually *less* intense than the multiparticle excitation terms by a factor of order Δq. For all these reasons, we believe that the single-particle excitations cannot be resolved in the scattering spectrum of *soft* x rays, unless of course some other agent relaxes momentum conservation. In that case, the range of interference in Eq. (14) would again be of atomic size.

III. INFRARED SINGULARITIES IN THE ABSENCE OF INTERFERENCE

A. Analysis of kernel for transition rate

We are interested in the same mechanism[4-6] that is responsible for the threshold singularities in x-ray absorption or emission, namely the interaction between the conduction electrons with the transient core hole. The conduction electron Hamiltonian is given by Eq. (8). We ignore the Coulomb interaction between electrons. It is understood that it has been included in a renormalization of ϵ_k and $V_{kk'}$. Typical diagrams contributing to S, the kernel of Eq. (11), are depicted in Fig. 3. They involve two open lines beginning in t, u' and ending in t', u—hence the two possibilities shown in Figs. 3(a) and 3(b). A bubble on a full electron line signifies any number of scatterings of the electron on either of the dotted core hole lines; the full line goes back and forth between the upper and lower time branches. In addition, the diagram may exhibit any number of closed loops which may be either constrained to one branch as in Fig. 3(a) or sitting across both branches as in Fig. 3(b). We recall that each line between branches corresponds to excitation of another particle (or hole) in the final state.

In this section we carry out the calculation of the transition rate W in the absence of interference, i.e., for $i=j$ in for example Eq. (14). Then W is given by Eq. (12) once we know the kernel S.

As for absorption,[4,6] the core hole has no internal structure and there is no memory between successive collisions with conduction electrons: The hole is either present or absent. Consequently, the linked-cluster theorem remains valid even though the scattering potential is transient and shared between the two time branches. Let L be

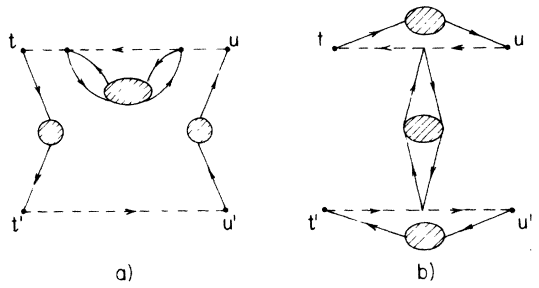

FIG. 3. Typical graphs contributing to the function $S(t, u, u', t')$.

the contribution of an open line and C the sum of all single closed loops. The kernel S may be written as

$$S(t, u, u', t') = [L(t, t')\, L(u', u) - L(t, u)\, L(u', t')]\, e^{C} \,. \tag{15}$$

The calculation of S ultimately reduces to that of the transient propagator $\phi(\tau, \tau')$ for a *single* particle in the transient scattering potential. Note that ϕ has four components since each of its extremities τ, τ' may be on either of the two branches.

B. Electron propagators, Dyson equations

For free electrons, the system has rotational symmetry around the single deep-hole site i which we choose as origin. We can then perform a partial wave expansion for all quantities, similar to that done in the absorption case.[6] The details may be found in Appendix A. In practice, that analysis of rotational symmetry is rather academic, since it breaks down in the spatial interference terms when $i \neq j$. For simplicity, then, we consider only one angular-momentum channel, say $l=0$, and we ignore complications arising from polarization and coherent scattering. Thus we assign the same matrix element w_k to the four electron-photon vertices of Fig. 3. We moreover assume that

$$w_k = w u_k \,, \qquad V_{kk'} = V u_k u_{k'} \,,$$

where u_k is an isotropic cutoff factor equal to one when $\epsilon_k = \epsilon_F$ and zero when $\epsilon = |\epsilon_k - \epsilon_F| \geq D$. This assumption of separability simplifies the algebra considerably, as it allows momentum sums to be performed at the outset. Every conduction electron operator c_k or $c_k^\dagger$ will have a u_k associated with it so that the electron propagator involves only the operator $\psi = \sum_k u_k c_k$.

In the Kjeldysh-Schwinger formalism the free-electron propagator has four components, depending upon in which time branches the extremities find themselves. These are defined in Fig. 4. Analytically,

$$G^-(\tau,\tau') = i\langle\psi(\tau)\psi^\dagger(\tau')\rangle = i\int_0^D \nu(\epsilon)u^2(\epsilon)e^{-i\epsilon(\tau-\tau')}d\epsilon\,, \tag{16a}$$

$$G^+(\tau,\tau') = -i\langle\psi^\dagger(\tau')\psi(\tau)\rangle = -i\int_{-D}^0 \nu(\epsilon)u^2(\epsilon)e^{-i\epsilon(\tau-\tau')}d\epsilon\,, \tag{16b}$$

$$G_c(\tau,\tau') = G^-(\tau,\tau')\Theta(\tau-\tau') + G^+(\tau,\tau')\Theta(\tau'-\tau)\,,$$

$$\tilde{G}_c(\tau,\tau') = G^-(\tau,\tau')\Theta(\tau'-\tau) + G^+(\tau,\tau')\Theta(\tau-\tau')\,. \tag{17}$$

Here $\nu(\epsilon)$ is the density of states of energy ϵ measured from ϵ_F and Θ is the usual step function.

Now let $\phi(\tau,\tau';\ t,u,t',t')$ be the full-electron propagator in the presence of the "intermediate state" interaction with the transient core hole: The electron may scatter any number of times with the hole on the upper branch in the interval (t,u) and/or on the lower branch in the interval (t',u'). The Dyson equations for the components of ϕ are easily written. For instance,

$$\phi_c(\tau,\tau') = G_c(\tau,\tau') + V\int d\tau''\,[G_c(\tau,\tau'')\eta(\tau'')\phi_c(\tau'',\tau') - G^+(\tau,\tau'')\eta'(\tau'')\phi^-(\tau'',\tau')]\,, \tag{18a}$$

$$\phi^-(\tau,\tau') = G^-(\tau,\tau') + V\int d\tau''\,[G^-(\tau,\tau'')\eta(\tau'')\phi_c(\tau'',\tau') - \tilde{G}_c(\tau,\tau'')\eta'(\tau'')\phi^-(\tau'',\tau')]\,. \tag{18b}$$

We have introduced functions $\eta(\tau)$ and $\eta'(\tau)$ equal to one in the ranges (t,u) and (t',u'), respectively, and zero elsewhere. Similar equations are obeyed by $\tilde{\phi}_c$ and ϕ^+.

C. Asymptotic approximation, Calculation of transition rate

The Eqs. (18) are exact. We now make the central approximation of our work: We assume that the times of interest $|\tau-\tau'|$ are long compared to the inverse bandwidth D^{-1} and we replace all the $G(\tau,\tau')$ by their asymptotic form in the limit $D|\tau-\tau'| \gg 1$. Any structure at short $|\tau-\tau'|$ is lumped into a δ function. Such an approximation is discussed in Ref. 6; it is only valid if both incident and scattered x rays are near threshold, i.e., $\omega, \omega' \ll D$.

Our asymptotic calculation can only pretend to determine the singular behavior *near* threshold—a quantitative estimate of the transition rate for large ω *or* ω' is outside its realm. For simplicity we assume particle-hole symmetry in the conduction band so that ν and u are even functions of ϵ (this is in no way essential and may be relaxed at the cost of extra algebra). We thus find, with $\epsilon = 0^+$,

$$G_c = \tilde{G}_c \approx \nu_0 P(1/\tau-\tau')\,, \qquad G^- = (G^+)^* \approx \nu_0/(\tau-\tau'-i\epsilon)\,. \tag{19}$$

When this result is used in Eqs. (18), we find a set of two coupled singular integral equations of the Mushkhelishvili type.[8]

Actually, the two coupled equations reduce to one, as follows:

Use Eq. (19) in Eqs. (18) and subtract the two equations. This leads to a relation between ϕ^- and ϕ_c.

$$[1+i\pi g\eta'(\tau)]\phi^-(\tau,\tau') = [1+\pi g\eta(\tau)]\phi_c(\tau,\tau') + i\pi\nu_0\delta(\tau-\tau')\,, \tag{20}$$

where $g = \nu_0 V$ is the dimensionless coupling constant. In this way, we eliminate ϕ^- and find that ϕ_c obeys

$$A(\tau)\phi_c(\tau,\tau') = -\frac{i}{\pi}\int d\tau''\,\frac{P}{\tau-\tau''}\times B(\tau'')\phi_c(\tau'',\tau') + f(\tau,\tau')\,, \tag{21}$$

where

$$A(\tau) = [1+\pi^2 g^2\eta(\tau)\eta'(\tau)]/[1+i\pi g\eta'(\tau)]\,, \qquad B(\tau) = i\pi g[\eta(\tau)-\eta'(\tau)]/[1+i\pi g\eta'(\tau)]\,, \tag{22}$$

$$\frac{f(\tau,\tau')}{\nu} = \frac{-\pi^2 g^2\eta'(\tau)}{1+i\pi g(\tau)}\delta(\tau-\tau') + P\frac{1}{\tau-\tau'}\,\frac{1}{1+i\pi g\eta'(\tau)}\,. \tag{23}$$

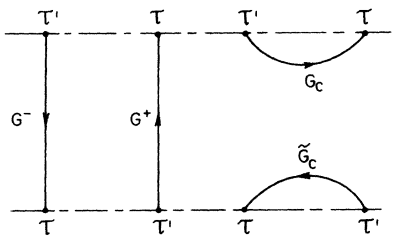

FIG. 4. The components of the free-particle propagator.

Equation (21) is of the standard Mushkhelishvili type. Its solution is given explicitly in section 108 of Ref. 8. We express the result in terms of the phase shift δ for electron–deep-hole scattering at the Fermi surface. In our model, $\tan\delta = \pi g$. We also define

$$\xi(\tau) = [(\tau - u)/(\tau - t)]^{\delta/\pi},$$

$$\xi'(\tau) = [(\tau - u')/(\tau - t')]^{\delta/\pi}. \tag{24}$$

The function ξ is defined with a branch cut from t to u, with $\arg \xi = +\epsilon$ above the cut and $\arg \xi = 0$ on the rest of the real axis. ξ' is defined similarly on the range (t', u'). Then the complete solution of Eqs. (18) and (19) may be written as follows:

$$\begin{aligned}
\frac{1}{\nu_0}\phi_c(\tau,\tau') &= P\frac{1}{\tau-\tau'}\,\mathrm{Re}\,\xi(\tau')\,\mathrm{Re}\,\frac{1}{\xi(\tau)}\,\frac{\xi'(\tau_+)}{\xi'(\tau'_+)} - \pi\delta(\tau-\tau')\sin\delta\cos\delta\,\eta(\tau),\\
\frac{1}{\nu_0}\phi^-(\tau,\tau') &= \frac{1}{\tau-\tau'-i\epsilon}\,\frac{\mathrm{Re}\,\xi(\tau')\,\mathrm{Re}\,\xi'(\tau)}{\xi(\tau_-)\,\xi'(\tau'_+)},\\
\frac{1}{\nu_0}\phi^+(\tau,\tau') &= \frac{1}{\tau-\tau'+i\epsilon}\,\mathrm{Re}\,\frac{1}{\xi(\tau)}\,\mathrm{Re}\,\frac{1}{\xi'(\tau')}\,\xi(\tau'_-)\,\xi'(\tau_+),\\
\frac{1}{\nu_0}\tilde\phi_c(\tau,\tau') &= P\frac{1}{\tau-\tau'}\,\mathrm{Re}\,\xi'(\tau)\,\mathrm{Re}\,\frac{1}{\xi'(\tau')}\,\frac{\xi(\tau'_-)}{\xi(\tau_-)} + \pi\delta(\tau-\tau')\sin\delta\cos\delta\,\eta'(\tau).
\end{aligned} \tag{25}$$

We note that the various components of ϕ are all singular when τ or τ' approach the edges of the interaction range t, u, t', or u'. Such singularities are due to the asymptotic approximation of Eq. (19); they are healed by introducing a time cutoff $\approx D^{-1}$ as in Ref. 6.

From the full transient propagator ϕ, it is now straightforward to obtain the open line and closed-loop contributions to S in Eq. (15) (our discussion parallels that of Ref. 6): We derive C with respect to the interaction strength V. This is equivalent to picking out any one vertex on either the upper or lower interaction ranges. Thus

$$V\frac{\partial C}{\partial V} = -iV\int_{-\infty}^{+\infty}[\phi_c(\tau,\tau)\eta(\tau) - \tilde\phi_c(\tau,\tau)\eta'(\tau)]\,d\tau. \tag{26}$$

Clearly, the asymptotic result [Eq. (25)] cannot be used here; in fact, it diverges for $\tau' = \tau$. We rather remark that when $\tau' \to \tau$, the product of transient factors ξ in Eq. (25) becomes a constant independent of t, u, t', u'. The reason is that on a short time scale, the propagator ϕ is the same as if the potential V were established *permanently* (a hardly surprising result!). In such a limit, C is related to the energy shift Δ of the electron ground state due to the static potential V; indeed, one verifies that

$$C_0 = -i\Delta(u - t - u' + t'). \tag{27}$$

When exponentiated, this zeroth-order contribution gives a shift in the threshold frequency ω_0, a rather obvious effect that we ignore by a redefinition of ω_0. The interesting features come from the transient factors ξ in Eq. (25). If we expand ξ, ξ' in powers of $\tau' - \tau$ and let $\tau' \to \tau$, we see that $\eta\phi_c(\tau,\tau)$ acquires a new contribution

$$\begin{aligned}
\eta(\tau)\,\delta\phi_c(\tau,\tau) = &-\nu_0\eta(\tau)\\
&\times\frac{\delta}{\pi}\left[\frac{1}{\tau_+ - t'} - \frac{1}{\tau_+ - u'}\right.\\
&\left.+ P\left(\frac{1}{\tau-u} - \frac{1}{\tau-t}\right)\right]\cos^2\delta.
\end{aligned}$$

A similar correction occurs for $\eta'\tilde\phi_c$. We insert these corrections into Eq. (26) and integrate to the cutoff D^{-1}. The resulting correction δC is given by

$$\frac{\partial C}{\partial g} = \frac{2\delta}{\pi}\cos^2\delta\,\ln\left(\frac{X}{D^2}\right), \tag{28}$$

where

$$X = \frac{u - t' + i\epsilon}{t - t' + i\epsilon}\,\frac{t - u' + i\epsilon}{u - u' + i\epsilon}\,\frac{1}{(u-t)(u'-t')}. \tag{29}$$

Since $\pi\cos^2\delta = \partial\delta/\partial g$, we find, from Eq. (28),

$$e^C = (X/D^2)^{\delta^2/\pi^2}. \tag{30}$$

We note that Eq. (30) has only logarithmic accuracy since the cutoff D is only known qualitatively.

Then open-line contribution [the bracket of Eq. (15)] is even simpler: It is equal to

$$|w|^2[\phi_c(u,t)\,\tilde\phi_c(t',u') - \phi^-(t',t)\,\phi^+(u,u')]. \tag{31}$$

Using Eq. (25), we find that[9]

$$\begin{aligned}
\phi_c(u,t)\,\tilde\phi_c(t',u') &= \frac{\nu_0^2}{(u-t)(t'-u')}\left(\frac{D^2}{X}\right)^{2\delta/\pi},\\
\phi^-(t',t)\,\phi^+(u,u') &= \frac{\nu_0^2}{(t'-t-i\epsilon)(u-u'+i\epsilon)}\left(\frac{D^2}{X}\right)^{2\delta/\pi}.
\end{aligned}$$

The net open-line contribution Eq. (31) is then equal to[10]

$$-\nu_0^2|w|^2 X(D^2/X)^{2\delta/\pi}. \tag{32}$$

Inserting Eqs. (30) and (32) into Eq. (5), we obtain our final result

$$S(t, u, u', t') = -\,|\,\nu_0 w\,|^2\, X^{1-n}\, D^{2n}\,, \tag{33}$$

with $\eta = 2\delta/\pi - \delta^2/\pi^2$. Remember that while the exponent n is exact, the cutoff D is only qualitatively defined.

With Eq. (33) the problem is solved; we need only Fourier transform S as in Eq. (19) to find the scattering cross section. Unfortunately, this last step is rather messy. Using Eq. (29), we have (up to a constant factor)

$$W(\omega, \omega') = \int_{-\infty}^{+\infty} du' \int_{-\infty}^{0} dt \int_{-\infty}^{u} dt'\; e^{i\omega(t'-t) - i\omega' u'} \left(\frac{t' - i\epsilon}{u' - i\epsilon}\,\frac{t - u' + i\epsilon}{t - t' + i\epsilon}\,\frac{1}{t(t' - u')}\right)^{1-n}. \tag{34}$$

We can check that the analytic structure of S is correct by the change of variable $t' \to v + u'$. Eq. (34) becomes

$$W(\omega, \omega') = \int_{-\infty}^{0} dt\, dv \int_{-\infty}^{+\infty} du'\; e^{i\omega(v-t)}\; e^{i(\omega-\omega')u'} \left(\frac{(u' + v - i\epsilon)(t' - u' + i\epsilon)}{(u' - i\epsilon)(t - v - u' + i\epsilon)\, tv}\right)^{1-n}.$$

Since the singularities in the u' plane are all above the real axis, this form guarantees that $W = 0$ if $\omega < \omega'$, a comforting conclusion. We perform a different change of variable, better suited to the actual determination of W: $t - t' = v'$, $u' - (t + t') = 2x$. Then, from Eq. (34),

$$W(\omega, \omega') = \int_{-\infty}^{+\infty} du'\, dv'\, f(u', v')\,[(u' - i\epsilon)(v' + i\epsilon)]^{n-1}\; e^{-i(\omega' u' + \omega v')}\,, \tag{35a}$$

$$f(u', v') = \int_{|u'+v'|/2}^{\infty} \{[4x^2 - (u' - v' - i\epsilon)^2]/[4x^2 - (u' + v')^2]\}^{1-n}\,. \tag{35b}$$

D. Fluorescence and scattering

The integrand of Eq. (35b) goes to 1 when $x \to \infty$, so that there is a divergence in f which can only be cured by introducing *ex abrupto* a damping factor $\exp(-\Gamma x) = \exp[-\frac{1}{2}\Gamma(u - t + u' - t')]$ into the integrand. We immediately see from this form that this corresponds to introducing a *finite lifetime for the deep hole*. This divergence, cured by lifetime effects, precisely corresponds to the fluorescence singularity we are looking for. Indeed, let us add and subtract 1 in the integrand of Eq. (35b) including the damping factor. We find

$$f(u', v') = \frac{1}{\Gamma} + \frac{1}{2}\,|\,u' + v'\,|\,\psi\!\left(\frac{u' - v' - i\epsilon}{|\,u' + v'\,|}\right) + O(\Gamma)\,, \tag{36a}$$

where

$$\psi(z) = \int_1^{\infty} \left[\left(\frac{x^2 - z^2}{x^2 - 1}\right)^{1-n} - 1\right] dx - 1\,. \tag{36b}$$

When inserted into Eq. (35a), the first term of f, $1/\Gamma$ gives the fluorescence contribution to the scattering rate:

$$W_F(\omega, \omega') = \theta(\omega)\omega^{-n}\;\theta(-\omega')w'^{-n}/\Gamma\,. \tag{37}$$

We see that W_F, as expected, is the product of the absorption probability $\propto \omega^{-n}$ $(\omega > 0)$, the emission probability $\propto \omega'^{-n}$ $(\omega' < 0)$ and the lifetime Γ^{-1}.[11]

Genuine Raman scattering W_R occurs only when ω, ω' have the same sign (the intermediate state is then virtual). Mathematically it arises from the second term of Eq. (36a). Since

$$W_R(\omega, \omega') = W_R(-\omega', \omega)$$

[let $u' \to -v'$, $v' \to -u'$ in Eqs. (35a) and (36)], we need only consider one case—say $0 < \omega' < \omega$. We evaluate Eq. (35a) using Eq. (36) and the variable change $a = \frac{1}{2}|\,u' + v'\,|$, $z = (u' - v')/|\,u' + v'\,|$. We find

$$W_R(\omega, \omega') = 4\,\mathrm{Re}\int_0^{\infty} a^{2n}\, da \int_{-\infty}^{+\infty} dz \times \frac{\psi(z - i\epsilon)}{[1 - (z - i\epsilon)^2]^{1-n}}\; e^{ia(\omega-\omega')(z-z_0)}\,, \tag{38}$$

where $z_0 = (\omega + \omega')/(\omega - \omega') > 1$. The a integral yields (within constant factors)

$$W_R(\omega, \omega') = 4\,\mathrm{Re}\int_{-\infty}^{+\infty} \frac{\chi(z - i\epsilon)\, dz}{[\epsilon - i(\omega - \omega')(z - z_0)]^{1+2n}}\,, \qquad \chi = \psi(1 - z^2)^{n-1}\,. \tag{39}$$

The last integral over z must be performed numerically. In Appendix B we reduce it to a *real* integral more suitable for computing. Here we only comment on general features:

(i) The Raman scattering rate is a homogeneous function of ω and ω' of degree $-(1 + 2n)$, i.e.

$$W_R(\omega, \omega') = \frac{1}{|\,\omega + \omega'\,|^{1+2n}}\, f\!\left(\frac{\omega'}{\omega}\right). \tag{40}$$

This was expected from dimensional arguments.[12] The infrared singularities are thus well marked.

(ii) If $\Delta\omega = \omega - \omega' \ll \omega$ (energy transfer small compared to the distance from threshold), z_0 is $\gg 1$. In Eq. (B3)[13] we expand $\lambda(z) = A + B/z^2 + \cdots$. Ultimately, we find

$$W_R(\omega, \omega') \sim \Delta\omega/\omega^{2+2n} . \tag{41}$$

The transition rate is proportional to the energy transfer $\Delta\omega$, a result that follows at once from the exclusion principle: The number of excited states having n electrons and n holes with net energy smaller than E goes as E^{2n}—hence a density of states $\propto E^{2n-1}$. For small $\Delta\omega$, the scattering is dominated by $n=1$. Then the density of final states is $\propto \Delta\omega$, while the matrix element for scattering is resonant, behaving as $1/\omega^{1+n}$; hence the result of Eq. (41).

(iii) If $\omega' \ll \omega$, z_0 is close to 1, the integral in Eq. (B3)[13] is dominated by the range $z \approx 1$, in which $\lambda(z) \approx \frac{1}{2}(z-1)^{n-1}$. We then find

$$W_R(\omega, \omega') \approx (1/\omega^n \omega'^{1+n}) . \tag{42}$$

The enhancement of W_R due to infrared singularities is evenly shared between the incident and scattered frequencies.

(iv) Between the limits (ii), (iii), a numerical solution of Eq. (B3) is required. A *qualitative* interpolation[14] that fits both limits is

$$W_R(\omega, \omega') \approx \frac{\omega - \omega'}{\omega\omega'} \frac{1}{\omega^n} \frac{1}{\omega'^n} . \tag{43}$$

It seems that the noninteracting electron result [first factor of Eq. (43)], is enhanced *separately* by the absorption (second factor) and emission (third factor) processes.

(v) We emphasize that these results are still very far from experiment. We have neglected the actual smearing due to finite lifetime and, more essential, we have ignored the interference effects [terms with $i \neq j$ in Eq. (14)]. In view of these limitations, it is not worthwhile to carry the calculations further.

IV. INTERFERENCE EFFECTS

A. Modification of propagators

We now turn to the interference terms which are described by the same diagrams of Fig. 2 where now the upper and lower core-hole lines correspond to different atomic sites i, j. Rotational symmetry is broken and we cannot decouple the different angular-momentum channels as in Appendix A—this precludes any precise quantitative calculation. We can nevertheless achieve some qualitative understanding by using the same separable interaction as in Sec. III: Momentum sums are performed at the outset; the channel separation is not a problem. From Fig. 4, we can see that the bare propagators G_c and $\tilde{G}_c$ are unaffected by the fact that $i \neq j$, since they propagate entirely on the upper and lower branches, respectively, in the presence of only one core hole: the one at i for G_c; the one at j for $\tilde{G}_c$. On the other hand, as we have discussed earlier in Sec. II [material following Eq. (12)], $G^{\pm}$ propagates between the two sites. We have

$$\begin{aligned} G^{-}_{ij}(t) &= i \sum_{k>k_F} u_k^2 \, e^{-i\epsilon_k t + i\vec{k}\cdot\vec{R}_{ij}} , \\ G^{+}_{ij}(t) &= -i \sum_{k<k_F} u_k^2 \, e^{-i\epsilon_k t + i\vec{k}\cdot\vec{R}_{ij}} . \end{aligned} \tag{44}$$

With this modification, the Dyson equations (18) for the transient propagator ϕ and the algebra leading to the kernel S [Eq. (15)] remain valid.

When t is much larger than the inverse bandwidth D^{-1}, $G^{\pm}_{ij}$ takes on its asymptotic form

$$G^{\pm}_{ij}(t) \approx \frac{\nu_0}{2ik_F R} \left(\frac{e^{ik_F R}}{t - R/v_F \pm i\epsilon} - \frac{e^{-ik_F R}}{t + R/v_F \pm i\epsilon} \right) , \tag{45}$$

where k_F, v_F are the Fermi momentum and velocity and $R = |R_{ij}|$. The $1/t$ behavior which is responsible for the infrared singularities, appears only when $t \gg R/v_F$, in which case

$$G^{\pm}_{ij} \approx \frac{D_0}{t \pm i\epsilon} \frac{\sin k_F R}{k_F R} . \tag{46}$$

In this asymptotic limit, the nonlocal nature of the interference terms shows up in two ways:

(i) a reduction factor $\alpha = \sin k_F R / k_F R < 1$ for each bare-electron line between the two branches of the diagram;

(ii) an increased cutoff R/v_F for those same lines, below which the asymptotic form Eq. (46) is invalid. If R is small (e.g., i and j nearest neighbors), then roughly $R/v_F \approx D^{-1}$, and this second effect is negligible in view of our crude treatment of the cutoff. On the other hand, the reduction α in the amplitude of $G^{\pm}$ has a drastic effect on the scattering rate and it deserves a more careful discussion.

Within this asymptotic, one-cutoff approximation, the transient propagators ϕ_c and ϕ^{-}_{ij} obey the same Eqs. (18) and (19), except that $G^{\pm}$ are everywhere multiplied by α. The Dyson equations are still two coupled singular integral equations of the Mushkhelishvili type, but unfortunately they no longer reduce to a single equation as they did when $\alpha = 1$. As a result, we were unable to solve them, despite the apparent simplicity of this 2×2 matrix problem.[15]

B. Limiting cases

Failing an exact solution, we looked for questions that we could answer. One possibility is to expand in powers of α, i.e., according to the numbers of lines $G^{\mp}$. Physically, this is an expansion in powers of the number of electrons and holes really excited in the scattering process. Final states with n electrons and n holes contribute a term $\propto \alpha^{2n}$ to S_{ij}. Such an expansion is meaningful when $|\omega - \omega'| \ll |\omega|$, since multiparticle excita-

tions are then restricted by the exclusion principle[16]: The scattering is dominated by $n=1$. The corresponding contribution to the interference term S_{ij} is the same as that to S_{ii} except for an extra factor α^2. Thus, for small energy transfer, we may transpose the former result [Eq. (41)] without further calculation. On the other hand, such an expansion in powers of α^2 is clearly very bad when $|\omega-\omega'|\approx\omega$, as it ignores the excitation of large numbers of electrons and holes (each with very small energy), which is known to be the major feature of infrared catastrophes. The first terms of the α^2 expansion can at best provide trends, not quantitative approximations. We nevertheless carried out the calculation of S and W to order α^2 in Appendix C. We find the expected result [Eq. (41)] if $|\omega-\omega'|<\omega$. In the opposite limit $0<\omega'\ll\omega$, the scattering rate $W(\omega,\omega')$ is reduced by a factor $\approx(\omega'/\omega)^{\delta^2/\pi^2}$ as compared to Eq. (42). While the general trend (reduction of the singularity in the interference terms at low ω') is probably correct, the precise result is not reliable.

C. Interference and fluorescence

Since we are unable to find the line shape of the scattered light [i.e., the precise ω, ω' dependence of $W(\omega,\omega')$], we may restrict our ambitions and ask only for the Γ dependence of W in the fluorescence region $\omega'<0<\omega$. This is not a matter of semantics only, as the very existence of the interference terms ($i\neq j$) in the case of fluorescence raises questions of principle. If we really have two real transitions in a row (separated roughly by a lifetime Γ^{-1}) between which a core hole exists at some *well-defined lattice site*, how can there be interference? What is questioned here is the very concept of a *real* intermediate state, as displayed by the singularity of $W(\omega,\omega')$ when $\Gamma\to 0$. This problem is of general interest, exceeding the framework of Raman scattering itself; it warrants a discussion in the present case where an explicit answer may be found.

In the case of interest, $\Gamma\ll\omega,-\omega'$ so that the transition rate $W(\omega,\omega')$, which is the transform of $S(t,u,u',t')$, is controlled by the behavior of S for large values of $x=\frac{1}{2}(u+u'-t-t')$. In fact, the important range is $x\gtrsim\Gamma^{-1}$, which is much larger than the other typical intervals $t-t'\approx\omega^{-1}$; $u-u'\approx\omega^{-1}$. The ω, ω', Γ dependences of W are thus decoupled since they depend on separate time variables—respectively $t-t'$, $u-u'$, x. If we look at the Γ dependence only, it is sufficient to know the x dependence of S for arbitrary values of the other variables. So we set $t=t'$, $u=u'$. Such a choice permits the solution of Eq. (18). The ω, ω' dependences of W involve the same difficulties we found for genuine Raman scattering.

The Dyson equations (18) can now be solved since we may set $\eta'(\tau)=\eta(\tau)$. As compared to Eq. (19), $G^{\pm}$ needs a factor α. If we define a two dimensional vector $\psi=(\phi_c,\phi^-)$, we may cast Eqs. (18) into a single vector equation

$$(1-i\pi g\alpha\sigma_1)\psi(\tau,\tau')=A+g\int_t^u d\tau''\,P\frac{1}{\tau-\tau''}(\sigma_3-i\alpha\sigma_2)\psi(\tau'',\tau')\,, \quad (47)$$

where the σ_i are the Pauli spin matrices and the inhomogeneous term A has components

$$\frac{A}{\nu_0}=P\left(\frac{1}{\tau-\tau'}\right)\begin{pmatrix}1\\ \alpha\end{pmatrix}+i\pi\delta(\tau-\tau')\begin{pmatrix}0\\ \alpha\end{pmatrix}.$$

The solution of Eq. (47) is straightforward and is given in Appendix D. It yields explicit expressions for ϕ_c and ϕ^-. From these we may find the open-line and closed-loop contributions to Eq. (15). Now it is clear that the open lines in Fig. 3(b) give a factor that vanishes when $x\to\infty$, while those of Fig. 3(a) remain finite. The former graphs are therefore negligible and in the latter, the x dependence arises entirely from the closed-loop factor e^C. Using the results of Appendix D, we find that

$$S(0,x,x,0)=1/x^{2\gamma^2/\pi^2}\,, \quad (48)$$

in which γ is an angle defined by

$$\tan^2\gamma=\pi^2g^2(1-\alpha^2)/(1+\pi^2g^2\alpha^2)\,. \quad (49)$$

It follows from Eq. (48) that in the fluorescence limit,

$$W(\omega,\omega')\approx 1/\Gamma^{1-2\gamma^2/\pi^2}\,. \quad (50)$$

We note that when $\alpha=1$ ($i=j$, identical sites), $\gamma=0$ in agreement with Sec. II [when $t=t'$, $u=u'$, Eq. (25) displays no infrared singularity]; in the opposite limit $\alpha\to 0$, $\gamma\to\delta$ (the phase shift).

We can now decide whether interference effects do or do not exist in the case of fluorescence. According to Eq. (50), the $i\neq j$ contributions to W are certainly negligible in the long lifetime limit ($\Gamma\to 0$), since they involve a weaker power of $1/\Gamma$ than the term $i=j$ [for which $W\propto 1/\Gamma$ of Eq. (37)]. If Γ increases, interference terms can in principle become important; however it is very likely that Eq. (50) is to be interpreted as a reduction of order $(\Gamma/\omega)^{2\gamma^2/\pi^2}$, or $(\Gamma/\omega')^{2\gamma^2/\pi^2}$, as compared to the $i=j$ term. In the framework of our calculation, such corrections are negligible—they would only be important in the transition region near threshold ($\omega,\omega'\lesssim\Gamma$) in which the distinction between Raman scattering and fluorescence becomes very vague. From this point of view, interference terms are no longer surprising in the fluorescence case; they correspond to the tail of the transition region. Because Γ is finite, the energy is not strictly conserved in the intermediate state and the latter is always slightly virtual. Thus there is a component of coherent Raman scattering for which interfer-

ence effects are to be expected. Whether the large number of interference terms $i \neq j$ can make up for the smallness of each is not clear. It seems likely that their influence can extend well beyond the transition region.

We note that the lack of interference effects in the limit $\Gamma \to 0$ is a consequence of final-state interactions: For free electrons, γ [Eq. (49)] would be zero and W would behave as $1/\Gamma$ for both $i=j$ and $i \neq j$. Interference terms would then be of major importance in the fluorescence process. This is not so surprising, since the incoming absorbed photon excites different atomic sites with a well-defined phase coherence. If this coherence persists until another photon is emitted, interference should take place. The fact that the absorption process is real is in a sense irrelevant. During the long lifetime Γ^{-1}, a resonance builds up between the incoming photon and the core excitation which in itself does not affect phase coherence; as long as it exists, the deep hole retains perfect phase memory. The latter can only be disrupted by inelastic processes (the final state interactions) that change the frequency of the wave function in a random way. If inelastic processes do occur, the phase fluctuations of different sites become uncorrelated after some time, the emitted photons are no longer coherent and interference disappears. The longer the lifetime, the more the phases have time to decorrelate themselves and therefore the more interference terms will be suppressed. This is just what we find; the inelastic processes arise from the final-state interactions of the deep hole with conduction electrons, the energy of the intermediate state is blurred, the frequency of the intermediate state undergoing random fluctuations. The possibility of interference is controlled by the correlation of the corresponding phases on atomic sites i and j. For $i=j$, the correlation is of course perfect and $\gamma=0$ [$\alpha=1$ in Eq. (49)]. When i and j are separated, the correlation is less and less perfect (γ increases) and interference disappears. Still, it takes a long lifetime to achieve this result as it is the frequency which fluctuates, not the phase itself.

The question posed at the beginning of this subsection is in fact answered by the observation that the experiment being described here, even in the case of fluorescence, does not measure the actual site of the core hole in the intermediate state. The excitations in the final state are not localized and in the absence of random processes (such as final state interactions) it would be an error not to add, with well-defined phases, the amplitudes of all processes (i.e., all localized core hole sites) which lead to the same final state.

In a sense, the above discussion is quite standard. However, it is not usual to view Raman scattering and fluorescence in this way and this is the main reason we went into it at some length. We are well aware that it does not provide concrete results that can be tested against experiment. For that, what we would need is an explicit calculation of $W_{ij}(\omega, \omega')$ for $i \neq j$ and for arbitrary ω/Γ and ω'/Γ; then we could discuss the influence of interference on the line shape, which is certainly essential. The formalism we used is perfectly suited for this problem. Unfortunately, we do not know how to solve the resulting equations, except by expansion methods which are clearly bad in the presence of infrared catastrophes. Hence we have only tried to provide partial answers that shed some light on the physics of the problem.

ACKNOWLEDGMENTS

One of us (P.N.) wishes to thank the Rutgers University Physics Department for its hospitality when this work was begun. The authors wish to acknowledge interesting conversations on the subject of this paper with J. L. Birman, S. Doniach, D. C. Langreth, P. M. Platzman, and C. S. Ting.

APPENDIX A

Here we discuss briefly the angular-momentum decoupling for the no-interference of Sec. III. Let (l_c, m_c) and (l_c', m_c') be the rotational quantum numbers of the upper and lower core hole lines in Fig. 3. To take full advantage of the resonance we require $l_c = l_c'$ (i.e., a single-core energy level); however, we may have $m_c \neq m_c'$. As a result, the four independent electron-photon vertices in Fig. 3 depend on m_c, m_c' and also the incoming and outgoing photon polarizations m_p, m_p'. Each matrix element may be expanded in spherical harmonics:

$$w_k(m_c, m_p) = \sum_{lm} w_{lm}(m_c, m_p)\ Y_{lm}(\hat{k})\ .$$

In this case, $l = l_c \pm 1$, $m = m_c + m_p$. One shows easily that l, m are good quantum numbers along each conduction electron line in the diagram. Therefore, the quantities L and C break into sums such as

$$C = \sum_{lms} C_l\ , \qquad L(t, t') = \sum_{lm} w_{lm}(m_c m_p)\, w_{lm}(m_c' m_p)\, L_l \tag{A1}$$

(s is the spin degree of freedom). The different spin and angular-momentum channels are decoupled, although dependent on m_c, m_c', m_p, m_p'. In this respect, the diagrams of Figs. 3(a) and 3(b) behave rather differently. In Fig. 3(a), one necessarily has $m_c = m_c'$; there is no interference in the scattering through different components of the core state. On the other hand, we may have $m \neq m'$, in which case the scattered light is partially de-

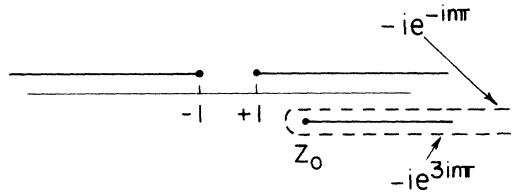

FIG. 5. Cuts for the integration of Eq. (39) when $\omega > \omega'$.

polarized. Indeed, it is totally depolarized if we select $l=0$ from Eq. (A1). In Fig. 3(b), the situation is reversed. Here $m=m'$; there is no depolarization. However, it is possible that $m_c \neq m_c'$ (coherent scattering by various core states; hence interference). We note that the latter processes only contribute to inelastic scattering when final-state interactions are included.

APPENDIX B

In the integral of Eq. (39), the denominator has a branch point at $z=z_0-i\epsilon/(\omega-\omega')$, which lies above the real axis if $\omega'>\omega$, below if $\omega>\omega'$. In contrast, the numerator $\chi(z)$ has two branch cuts extending from $\pm 1+i\epsilon$ to $\pm\infty$, fully above the real axis. If $\omega<\omega'$ all singularities are above and by closing the contour below, we find $W(\omega<\omega')=0$, as expected. In the other case, $\omega>\omega'$, the cuts are depicted in Fig. 5. Before deforming the contour, we note that we may add a constant to $\chi(z-i\epsilon)$ without affecting the integral (the corresponding integrand is analytic in the upper half plane). Therefore we replace $\chi(z)$ by $\chi(z)-\chi(z_0)$, which heals the singularity near $z=z_0$. We then deform the contour to a hairpin around the lower cut as shown by the dotted line in Fig. 5. The phases of the denominator are shown on the figure. Equation (39) becomes

$$W_R(\omega,\omega')=\frac{-8}{(\omega-\omega')^{1+2n}}\,\mathrm{Re}\int_{z_0}^{\infty}dz \times\frac{\chi(z-i\epsilon)-\chi(z_0-i\epsilon)}{|z-z_0|^{1+2n}}\,e^{-in\pi}\sin 2\pi n\,. \quad \text{(B1)}$$

For $z\geq z_0>1$, we have

$$\mathrm{Re}\,\chi(z-i\epsilon)\,e^{-in\pi}=\frac{\mathrm{Re}\,\psi(z-i\epsilon)}{|z^2-1|^{1-n}}\,. \quad \text{(B2)}$$

Now, $\psi(z)$ is given by Eq. (36b), the integrand of which has branch cuts in the complex x plane as shown in Fig. 6. To calculate $\mathrm{Re}\psi$, we consider

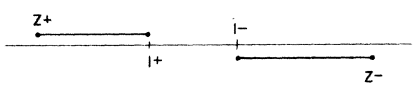

FIG. 6. Cuts for the integration of Eq. (36b).

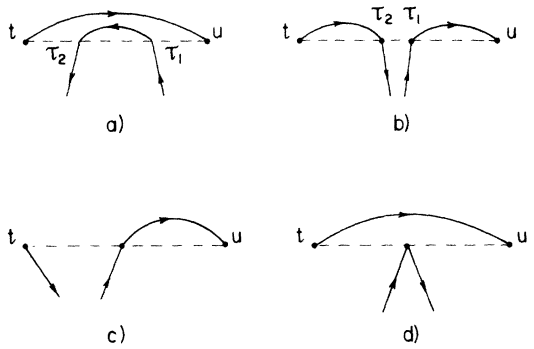

FIG. 7. Structure of graphs when interference effects are included.

the integral

$$I=\int_{-\infty}^{+\infty}\left[\left(\frac{x^2-z^2}{x^2-1}\right)^{1-n}-1\right]dx\,.$$

We may evaluate I either by splitting the integration range into $(0,1)$ and $(1,\infty)$ or by closing the contour around the lower cut. We then find

$$\psi(z-i\epsilon)=-\int_0^1\left(\frac{z^2-x^2}{1-x^2}\right)^{1-n}dx+i\sin\pi n \times\int_1^z\left(\frac{z^2-x^2}{1-x^2}\right)^{1-n}dx\,.$$

Equation (B1) for W takes the form (within constant factors)

$$W_R(\omega,\omega')=W_R(-\omega',-\omega) \approx\frac{1}{|\omega-\omega'|^{1+2n}}\int_{z_0}^{\infty}\frac{\lambda(z)-\lambda(z_0)}{(z-z_0)^{1+2n}}dz\,, \quad \text{(B3)}$$

$$\lambda(z)=\frac{1}{(z^2-1)^{1-n}}\int_0^1\left(\frac{z^2-x^2}{1-x^2}\right)^{1-n}dx\,,$$

$$z_0=(\omega+\omega')/(\omega-\omega')\,.$$

The integrals of Eq. (B3) must be found numerically. Equation (B3) is the most explicit form of our result.

APPENDIX C

We want to calculate that part of $S(t,u,u',t')$—and of $W(\omega,\omega')$—that is of order α^2, i.e., which arises from diagrams containing only *one* line $G^-(\tau_1',\tau_1)$ and only *one* line $G^+(\tau_2,\tau_2')$. Such graphs split into an upper and a lower part connected only by the two cross lines G^+, G^-. Consider the upper part, which contributes to S a factor $F(t,u,\tau_1,\tau_2)$. The open lines may be arranged in two ways, shown in Figs. 7(a) and 7(b). In addition, some of the external points t, u, τ_1, τ_2 may coalesce as shown, for example, in Figs. 7(c) and 7(d). Altogether, $F(t,u,\tau_1,\tau_2)$ is given by

$$F(t,u,\tau_1,\tau_2)=e^{\bar{C}}\{\bar{\phi}_c(t,u)\times[V\delta(\tau_1-\tau_2)+V^2\bar{\phi}_c(\tau_1,\tau_2)]-[\delta(t-\tau_2)+V\bar{\phi}_c(t,\tau_2)]\times[\delta(\tau_1-u)+V\bar{\phi}_c(\tau_1,u)]\}\ , \tag{C1}$$

where $\bar{\phi}_c$ is the transient propagator in the presence of the upper branch core-hole potential only [scattering within (t,u) and no excursions to the lower branch] and $\bar{C}(u,t)$ denotes the closed-loop contribution with the same restriction. The quantities $\bar{\phi}_c$, $\bar{C}$ have been obtained previously in the study of x-ray absorption.[6] They are

$$\frac{1}{\nu_0}\bar{\phi}_c(\tau_1,\tau_2)=P\frac{1}{\tau_1-\tau_2}\,\mathrm{Re}\xi(\tau_2)\times\mathrm{Re}\frac{1}{\xi(\tau_1)}-\pi\delta(\tau_1-\tau_2)\sin\delta\cos\delta\,\eta(\tau_1)\ ,$$
$$e^{\bar{C}}=\left(\frac{D}{u-t}\right)^{\delta^2/\pi^2}\ , \tag{C2}$$

where $\xi(\tau)$ is defined in Eq. (24). Let $F'(t',u',\tau_1',\tau_2')$ be the similar contribution from the lower part of the full graph.

To order α^2, we find that

$$S(t,u,u',t')=\alpha^2\int_t^u d\tau_1\,d\tau_2\int_{t'}^{u'}d\tau_1'\,d\tau_2'\,F(t,u,\tau_1,\tau_2)\,F'(t',u',\tau_1',\tau_2')\,G^-(\tau_1-\tau_1')\,G^+(\tau_2'-\tau_2)\ . \tag{C3}$$

We Fourier expand $G^{\mp}$ according to Eqs. (16). F appears in the expression

$$\int_t^u F(t,u,\tau_1,\tau_2)\,e^{i(\epsilon_1\tau_1-\epsilon_2\tau_2)}\,d\tau_1\,d\tau_2=e^{i(\epsilon_1-\epsilon_2)t}\,F(\epsilon_1,\epsilon_2,u-t)\ . \tag{C4}$$

We use Eq. (C3) in Eq. (12) and find

$$W(\omega,\omega')=2\pi\alpha^2\int_0^D\nu_1\,d\epsilon_1\int_{-D}^0\nu_2\,d\epsilon_2\,|B|^2\,\delta(\omega-\omega'-\epsilon_1+\epsilon_2)\ , \tag{C5}$$

where

$$B=B(\epsilon_1,\epsilon_2,\omega')=\int_0^\omega e^{i\omega' x}\,F(\epsilon_1,\epsilon_2,x)\,dx \tag{C6}$$

[we set $u(\epsilon_1)=u(\epsilon_2)=1$]. In Eq. (C5), we recognize the usual Golden Rule, where $\alpha B(\epsilon_1,\epsilon_2,\omega')$ is an *effective matrix element* for one particle-one hole excitation, taking into account all many-body-effects in the scattering amplitude.

Combining Eqs. (C1)–(C6), we see that the calculation of $W(\omega,\omega')$ is reduced to a series of quadratures (rather messy, actually), the behavior of which can be estimated in limiting cases. We do not pursue this point further, the purpose of this Appendix being to stress the idea of an effective matrix element.

APPENDIX D

In Eq. (47), let us set

$$(1-i\pi g\alpha\sigma_1)\,\psi=\psi'\ .$$

Then ψ' obeys the integral equation

$$\psi'(\tau)=A(\tau)+g\int_t^u d\tau''\ P\left(\frac{1}{\tau-\tau''}\right)B\psi'(\tau'')\ , \tag{D1}$$

in which

$$B=(\sigma_3-i\alpha\sigma_2)\left(\frac{1+i\pi g\alpha\sigma_1}{1+\pi^2g^2\alpha^2}\right)\ . \tag{D2}$$

The eigenvalues of B are easily found; they are

$$\pm\left(\frac{1-\alpha^2}{1+\pi^2g^2\alpha^2}\right)^{1/2}=\pm\lambda\ .$$

Thus, there exists a constant matrix U such that

$$UBU^{-1}=\lambda\sigma_3\ . \tag{D3}$$

If we set $\psi''=U\psi'$, we find that Eq. (D1) becomes

$$\psi''(\tau)=UA(\tau)+\lambda g\int_t^u d\tau''\ P\left(\frac{1}{\tau-\tau''}\right)\sigma_3\psi''(\tau'')\ . \tag{D4}$$

The matrix integral equation (47) is thereby diagonalized. The solution to Eq. (D4) is found explicitly in Ref. 8 and is given by

$$\psi''(\tau,\tau')=a\,P\left(\frac{1}{\tau-\tau'}\right)+b\delta(\tau-\tau')\ ,$$

in which a, the only coefficient of interest to us, turns out to be

$$a=\nu_0\cos^2\gamma\begin{pmatrix}\zeta(\tau')/\zeta(\tau) & 0\\ 0 & \zeta(\tau)/\zeta(\tau')\end{pmatrix}U\begin{pmatrix}1\\ \alpha\end{pmatrix}+\frac{\nu_0\sin\gamma\cos\gamma}{\pi}\begin{pmatrix}\zeta(\tau')/\zeta(\tau) & 0\\ 0 & -\zeta(\tau')/\zeta(\tau)\end{pmatrix}U\begin{pmatrix}0\\ -i\pi\alpha\end{pmatrix}\ . \tag{D5}$$

In Eq. (D5), the angle γ is defined by $\tan\gamma=\pi\lambda g$ and the quantity $\zeta(\tau)=[(u-\tau)/(\tau-t)]^{\gamma/\pi}$ differs from ξ [Eq. (24)] by the replacement $\delta\to\gamma$. Equation (D5) is only valid if $\eta(\tau)\,\eta(\tau')=1$. From ψ'' we go back to ψ and find

$$\psi = \frac{1 + i\pi g \alpha \sigma_1}{1 + \pi^2 g^2 \alpha^2} U^{-1} \psi'' \ . \tag{D6}$$

Combining Eqs. (D5) and (D6) and making use of Eq. (D3), we finally obtain

$$(\tau - \tau')\psi(\tau, \tau') = \frac{\nu_0}{2(1+\pi^2 g^2)} \left\{ \left[\frac{\zeta(\tau)}{\zeta(\tau')} + \frac{\zeta(\tau')}{\zeta(\tau)} \right] \begin{pmatrix} 1 \\ \alpha \end{pmatrix} + \left[\frac{\zeta(\tau')}{\zeta(\tau)} - \frac{\zeta(\tau)}{\zeta(\tau')} \right] \begin{pmatrix} \lambda \\ -i\pi\alpha g \lambda \end{pmatrix} \right\} . \tag{D7}$$

In this way, we find $\psi = (\phi_c, \phi^-)$ and by a similar argument $(\bar{\phi}_c, \phi^+)$.

The closed-loop contribution C is given by Eq. (26); it involves $\phi_c(\tau, \tau)$. Were it not for the singular factors ζ in Eq. (D7), C would vanish. If however we expand $\zeta(\tau)/\zeta(\tau')$ in powers of $(\tau - \tau')$, we find that $\phi_c(\tau, \tau)$ and $\bar{\phi}_c(\tau, \tau)$ acquire a new "transient" term

$$\delta\phi_c(\tau, \tau) = -\delta\bar{\phi}_c(\tau, \tau) = \frac{\lambda\gamma/\pi\nu_0}{1+\pi^2 g^2} \left(\frac{1}{\tau - t} + \frac{1}{u - \tau} \right) , \tag{D8}$$

from which we obtain

$$\frac{\partial C}{\partial g} = \frac{-4\lambda\gamma}{\pi(1+\pi^2 g^2)} \ln[D(u-t)] , \tag{D9}$$

$$= \frac{-4}{\pi^2} \gamma \frac{d\gamma}{dg} \ln[D(u-t)] . \tag{D9}$$

The result in Eq. (48) follows at once. We do not give further details on this calculation as it is identical to that done for x-ray absorption.[6]

*Visitor at Rutgers University, 1972, where this research was begun and was supported by NSF grant GU-1592

†Work partially supported by NSF grant GH-36020.

[1]S. Doniach, P. M. Platzman, and J. T. Yue, Phys. Rev. B 4, 3345 (1971).

[2]J. T. Yue and S. Doniach, Phys. Rev. B 8, 4578 (1973).

[3]T. McMullen and B. Bergersen, Can. J. Phys. 50, 1002 (1972).

[4]B. Roulet, J. Gavoret, and P. Nozières, Phys. Rev. 178, 1072 (1969); P. Nozières, J. Gavoret, and B. Roulet, *ibid.* 178, 1084 (1969).

[5]C. S. Ting, J. L. Birman, and E. Abrahams, Solid State Comm. 10, 1101 (1972).

[6]P. Nozières and C. T. de Dominicis, Phys. Rev. 178, 1097 (1969).

[7]L. V. Kjeldysh, Zh. Eksp. Teor. Fiz. 47, 515 (1964) [Sov. Phys.-JETP 20, 1018 (1965)].

[8]N. I. Mushkhelishvili, *Singular Integral Equations* (Nordhoff, Groninger, 1953), Chap. 14.

[9]In calculating say $\phi_c(u, t)$, there is some ambiguity as to whether $\tau \to u$, $\tau' \to t$ from the inside or outside of the interval (t, u). The former choice implies an extra factor $\cos^2\delta$ as compared to the latter. Such an uncertainty, involving only a real factor, is unimportant in view of the qualitative nature of the cutoff. We make a consistent choice everywhere: τ, τ' are outside (t, u).

[10]That the two terms $\phi_c\bar{\phi}_c$ and $\phi^-\phi^+$ combine in such a way as to give the simple result of Eq. (32) is a consequence of our simple model involving a *single* angular-momentum channel. In the general case, cross terms with different (l, m) make the open-line contribution to S definitely more complicated.

[11]One may remark that in the diagrammatic representation, fluorescence arises from those graphs which split in two disconnected parts, one located near (t, t'), the other near (u, u').

[12]Refer to Eq. (37): The net degree in powers of ω, ω', Γ or equivalently, of the inverse cutoff, is the same as in Eq. (40).

[13]See Appendix B.

[14]That Eq. (43) is not the exact result can be seen by considering the case $n = \frac{1}{2}$, in which the solutions may be found explicitly in terms of elliptic functions.

[15]As shown in Ref. 8, Chap. 18, these equations are equivalent to a Hilbert problem for a two-dimensional vector $\Phi(z)$ which obeys the functional relation $\Phi(t + i\epsilon) = G(t)\,\Phi(t - i\epsilon) + A(t)$. $G(t)$ is a 2×2 matrix which depends only on $\eta(\tau)$ and $\eta'(\tau)$. If the matrix G could be written in the form $G(t) = X(t + i\epsilon)/X(t - i\epsilon)$, where $X(z)$ is analytic everywhere except the real axis, then the solution of Eqs. (18) would be straightforward. Such a decomposition of G, obvious in the one-component case, cannot be found in closed form for a 2×2 matrix.

[16]See the discussion following Eq. (41).